Global investigation of odd-even mass differences and radii with isospin-dependent pairing interactions

C. A. Bertulani,[1,*] Hongliang Liu,[1] and H. Sagawa[2]
[1]*Department of Physics, Texas A&M University—Commerce, Commerce, Texas 75429, USA*
[2]*Center for Mathematics and Physics, University of Aizu, Aizu-Wakamatsu, Fukushima 965-8580, Japan*
(Received 16 November 2011; published 24 January 2012)

Neutron and proton odd-even mass differences are systematically studied with Hartree-Fock (HF) + BCS calculations with Skyrme interactions and an isospin-dependent contact pairing interaction. The strength of pairing interactions is determined to reproduce empirical odd-even mass differences in a wide region of the mass table. By using the optimal parameter sets for proton and neutrons, we perform global (HF) + BCS calculations with Skyrme interactions and an isospin-dependent contact pairing interaction. The strength of pairing interactions is determined to reproduce empirical odd-even mass differences in a wide region of the mass table. By using the optimal parameter sets for proton and neutrons, we perform global HF + BCS calculations of nuclei and compare them with experimental data. The importance of the isospin dependence of the pairing interaction is singled out for odd-even mass differences in medium and heavy isotopes. Proton and neutron radii are studied systematically using the same model.

DOI: 10.1103/PhysRevC.85.014321 PACS number(s): 21.30.Fe, 21.60.−n

I. INTRODUCTION

Microscopic theories for calculating nuclear masses and/or binding energies (see, e.g., [1–3]) have been revived and further elaborated with the advance of computational resources. These advances are now sufficient to perform global studies based on, e.g., self-consistent mean-field theory, sometimes also denoted density functional theory [4,5]. One particular aspect of the nuclear binding problem is the phenomenon of odd-even staggering (OES) of the binding energy. Numerous microscopic calculations have been published that treat individual isotope chains. The mass number dependence of nuclear pairing was also studied using a Hartree-Fock-Bogoliubov (HFB) model with a finite-range Gogny interaction [6]. However, it might be necessary to examine the whole body of OES data to draw general conclusions [7].

Theoretically, OES values are often inferred from the average Hartree-Fock (HF) + BCS or HFB gaps [8–10], rather than directly calculated from the experimental binding energy differences between even and odd nuclei. It is worth mentioning that the average HFB gaps are in some cases substantially different from the odd-even mass differences calculated from experimental binding energies. In this work, we compare directly the calculated OESs with those extracted from experiment. In the literature there are several prescriptions for obtaining the OES from experiments, such as three-point, four-point, and five-point formulas [2,7,8]. Here we adopt the three-point formula $\Delta^{(3)}$ centered at an odd nucleus, i.e., odd-N nucleus for neutron gap and odd-Z nucleus for proton gap [2,7]:

$$\Delta^{(3)}(N,Z) \equiv \frac{\pi_{A+1}}{2}[\mathrm{B}(N-1,Z)-2\mathrm{B}(N,Z) + \mathrm{B}(N+1,Z)], \tag{1}$$

where $\mathrm{B}(N,Z)$ is the binding energy of the (N,Z) nucleus and $\pi_A = (-)^A$ is the number parity with $A = N + Z$.

For even nuclei, the OES is known to be sensitive not only to the pairing gap, but also to mean-field effects, i.e., shell effects and deformations [7,8]. Therefore, comparison of a theoretical pairing gap with OES should be done with some discretion. One advantage of $\Delta_o^{(3)}$ [$N =$ odd in Eq. (1)] is the suppression of the contributions from the mean field to the gap energy. Another advantage of $\Delta_o^{(3)}(N,Z)$ is that it can be applied to more experimental mass data than the higher order OES formulas. At a shell closure, the OES [Eq. (1)] does not go to 0 as expected, but it increases substantially. This large gap is an artifact owing to the shell effect, which is completely independent of the pairing gap itself.

An effective isospin-dependent pairing interaction has been proposed from the study of nuclear matter pairing gaps calculated with realistic nucleon-nucleon interactions. In Ref. [9], the density-dependent pairing interaction was defined as

$$V_{\mathrm{pair}}(1,2) = \mathrm{V}_0\, \mathrm{g}_\tau[\rho, \beta\tau_z]\, \delta(\mathbf{r}_1 - \mathbf{r}_2), \tag{2}$$

where $\rho = \rho_n + \rho_p$ is the nuclear density and β is the asymmetry parameter $\beta = (\rho_n - \rho_p)/\rho$. The isovector (IV) dependence is introduced through the density-dependent term g_τ. The function g_τ is determined by the pairing gaps in nuclear matter and its functional form is given by

$$\mathrm{g}_\tau[\rho, \beta\tau_z] = 1 - \mathrm{f_s}(\beta\tau_z)\eta_\mathrm{s}\left(\frac{\rho}{\rho_0}\right)^{\alpha_\mathrm{s}} - \mathrm{f_n}(\beta\tau_z)\eta_\mathrm{n}\left(\frac{\rho}{\rho_0}\right)^{\alpha_\mathrm{n}}, \tag{3}$$

where $\rho_0 = 0.16\ \mathrm{fm}^{-3}$ is the saturation density of symmetric nuclear matter. We choose $\mathrm{f_s}(\beta\tau_z) = 1 - \mathrm{f_n}(\beta\tau_z)$ and $\mathrm{f_n}(\beta\tau_z) = \beta\tau_z = [\rho_\mathrm{n}(\mathbf{r}) - \rho_\mathrm{p}(\mathbf{r})]\tau_z/\rho(\mathbf{r})$. The parameters for g_τ are obtained from the fit to the pairing gaps in symmetric and neutron matter obtained by the microscopic nucleon-nucleon interaction.

*carlos_bertulani@tamu-commerce.edu

In the literature and in many mean-field codes publicly available such as the original EV8 code [11], a pure contact interaction is used without an isospin dependence. In our notation, this amounts to replacing the isospin-dependent function g_τ in Eq. (2) with the isoscalar (IS) function

$$g_s = 1 - \eta_s \left(\frac{\rho}{\rho_0}\right)^{\alpha_s}. \tag{4}$$

The EV8 code has been modified, using the filling approximation, to account for mass calculations for odd-N and odd-Z nuclei and is publicly available as the EV8odd code [12]. It has also been modified to include isospin-dependent paring, by means of Eq. (2). The parameters of the IS interaction were adjusted with EV8 to the best global fit of nuclear masses [13]. They correspond to a surface peaked pairing interaction [Eq. (4) with η_s not too far from unity].

A recent publication has explored the isospin dependence of the pairing force for the OES effect for a few selected isotopic and isotonic chains [14]. Here we have made a more ambitious study by extending the calculation to the whole nuclear chart. We have also explored several other observables such as neutron and proton radii systematically, which may allow for more solid conclusions on isospin-dependent pairing interactions.

This paper is organized as follows. In Sec. II we discuss our numerical calculation strategy. Our results are presented in Sec. III for the energies, separation energies, OES energies, and nuclear radii. Our conclusions are presented in Sec. IV.

II. CALCULATION STRATEGY

HF + BCS calculations are performed using the SLy4 Skyrme interaction, which was found to be the most accurate interaction for studying OES for a few selected ($N = 50, 82$) isotonic and (Sn and Pb) isotopic chains [14]. Our iteration procedure used in connection with EV8odd achieves an accuracy of about 100 keV or less, with 500 HF iterations for each nuclear state. Our calculations were performed with the now decommissioned XT4 Jaguar supercomputer at ORNL, as part of the UNEDF-SciDAC-2 collaboration [15].

HF + BCS calculations were first performed for even-even nuclei. The variables in the theory are the orbital wave functions ϕ_i and the BCS amplitudes v_i and $u_i = \sqrt{1 - v_i^2}$. By solving the BCS equations for the amplitudes, one obtains the pairing energy from

$$E_{\rm pair} = \sum_{i \neq j} V_{ij} u_i v_i u_j v_j + \sum_i V_{ii} v_i^2, \tag{5}$$

where V_{ij} are the matrix elements of the pairing interaction, Eq. (2), namely,

$$V_{ij} = V_0 \int d^3r |\phi_i(\mathbf{r})|^2 |\phi_j(\mathbf{r})|^2 g_\tau[\rho(\mathbf{r}), \beta(\mathbf{r})\tau_z],$$

where $\rho(\mathbf{r}) = \sum_i v_i^2 |\phi_i(\mathbf{r})|^2$.

After determining the single-particle energies of even-even nuclei, the odd-A nuclei are calculated with the so-called filling approximation for the odd particle starting from the HF + BCS solutions of neighboring even-even nuclei: ones selects a pair of i and $\tilde{i}$ orbitals to be blocked and changes the BCS parameters v_i^2 and $v_{\tilde{i}}^2$ for these orbitals. The change is to set $v_i^2 = v_{\tilde{i}}^2 = 1/2$ in Eq. (5) for the pairing energy at an orbital near the Fermi energy. Note that this approximation gives equal occupation numbers to both time-reversed partners and does not account for the effects of time-odd fields. More details of the procedure are presented in Ref. [13].

The effect of time-odd HF fields on the mass were studied in Refs. [16,17]. It was pointed out that the effect of the time-odd fields is of the order of 100 keV for the binding energy, depending strongly on the configuration of the last particle, and does not show any clear sign of isospin dependence. Thus the time-odd field might not change the conclusions of the present study in the following, while quantitative accuracy might require some fine-tuning of the pairing parameters.

For the pairing channels we have taken the surface-type contact interaction, Eq. (4), and the isospin-dependent interaction, Eq. (3). The density dependence of the latter one is essentially the mixed-type interaction between the surface and the volume types. The pairing strength V_0 depends on the energy window adopted for BCS calculations. The odd nucleus is treated in the filling approximation, by blocking one of the orbitals. The blocking candidates are chosen within an energy window of 10 MeV around the Fermi energy. This energy window is rather small, but it is the maximum allowed by the EV8odd program. It is shown that the BCS model used in the EV8odd code gives results almost equivalent to those of the HFB model with a larger energy window, except for unstable nuclei very close to the neutron drip line [13]. The pairing strengths V_0 for IS and IS + IV pairing interactions are adjusted to give the best fit to OES of nuclear masses in a wide region of the mass table.

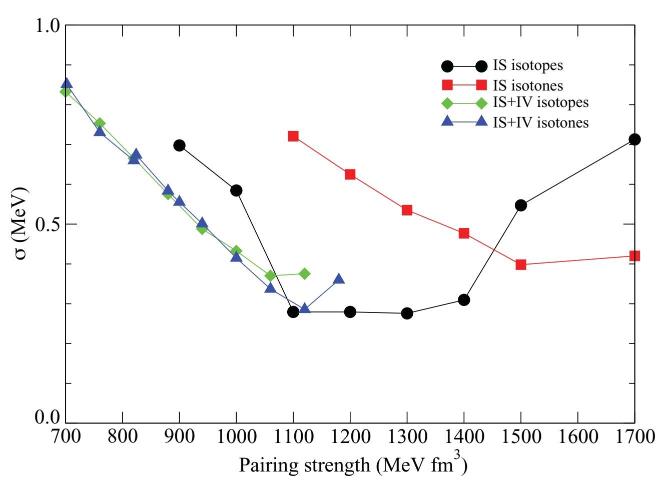

FIG. 1. (Color online) Mean square deviation σ of OES between experimental data and HF + BCS calculations. Filled circles and squares correspond to the results with IS pairing for neutron and proton gaps, respectively, while filled diamonds and triangles are those with IS + IV pairing for neutron and proton gaps. Experimental data are taken from Ref. [18]. See text for details.

TABLE I. Parameters for the density-dependent function g_τ defined in Eqs. (2) and (3) for the IS + IV interaction (first row) and g_s in Eq. (4) for the IS interaction. Parameters for g_τ are obtained from the fit to the pairing gaps in symmetric and neutron matter obtained with the microscopic nucleon-nucleon interaction. The paring strength V_0 is adjusted to give the best fit to odd-even staggering of nuclear masses. Parameters for g_s correspond to a surface peaked pairing interaction with no isospin dependence.

Interaction	V_0 (MeV fm^3)	ρ_0 (fm^{-3})	η_s	α_s	η_n	α_n
g_τ						
Isotopes	1040	0.16	0.677	0.365	0.931	0.378
Isotones	1120	0.16	0.677	0.365	0.931	0.378
g_s						
Isotopes	1300	0.16	1.	1.	–	–
Isotones	1500	0.16	1.	1.	–	–

III. NUMERICAL RESULTS

A. Global data on odd-even staggering

The results for the mean square deviation of our global mass table calculations are shown in Fig. 1. Table I lists the values V_0 in Eq. (2) and the parameters for g_τ and g_s in Eqs. (3) and (4) used in the present work. Optimal pairing strength values were found to be different for isotones (varying Z, constant N) and for isotopes (varying N, constant Z).

Figure 1 shows the mean square deviation σ of OES between experimental data and HF + BCS calculations. The mean square deviation σ is defined as

$$\sigma = \sqrt{\sum_{i=1}^{N_i} \left|\Delta_i^{(3)}(\mathrm{HF+BCS}) - \Delta_i^{(3)}(\exp)\right|^2 / N_i}, \qquad (6)$$

where N_i is the number of data points. For the IS interaction, the results for neutrons show a shallow minimum at $V_0 \sim$ (1100–1300) MeV fm^3. For protons, the minimum becomes about $V_0 \sim 1500$ MeV fm^3. This difference makes it difficult to determine a unique pairing strength common for both neutrons and protons. The results of IS + IV pairing show a minimum at $V_0 \sim 1100$ MeV fm^3 for both neutron and proton OES, which makes it easier to determine the value for the pairing strength. Adopted values for the following calculations are listed in Table I. The optimal values V_0 for protons are slightly larger than those for neutrons. This is somewhat different from a naive understanding of the proton pairing channels in which the two-body Coulomb interaction may quench the paring correlations so that the proton pairing gaps are smaller than the neutron ones. Thus it is still an open question how large the effect of two-body Coulomb interaction is on the pairing gaps, although some theoretical studies have been done to figure it out by HFB calculations [19,20]. There is also another open question: whether or not the effect of Coulomb interaction is renormalizable in the pairing strength V_0 for protons. Because of these open questions, we keep the different values of V_0 for protons and neutrons in the present study. The validity of the global fit with one unique parameter for the pairing strength V_0 is an interesting open question for future study.

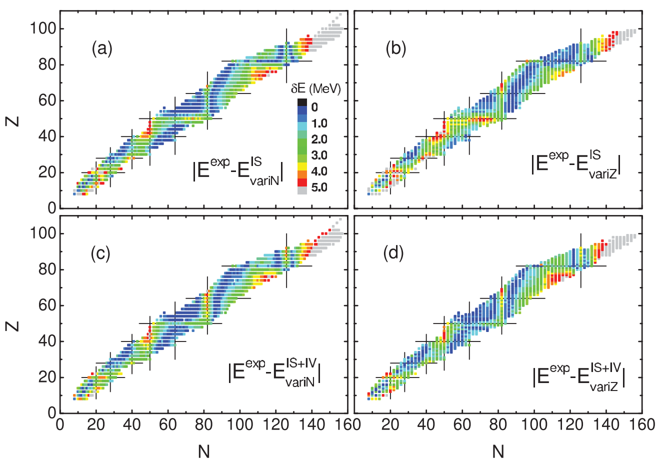

FIG. 2. (Color online) Binding energy differences between experimental data and calculations using the HF + BCS model with IS and IS + IV pairing interactions. (a), (c) Differences for even-Z isotones varying neutron numbers including both odd and even numbers. (b), (d) Differences for even-N isotones varying proton numbers including both odd and even numbers. Thin lines show the closed shells at $N(Z) = 20$, 28, 40, 50, 64, 82, and 126. Experimental data are taken from Ref. [18]. See text for details.

Systematic study of HF + BCS calculations are performed for various isotopes and isotones for all available data sets with ($Z = 8, \ldots, 102$) and ($N = 8, \ldots, 156$), respectively. Binding energy differences between experimental data and

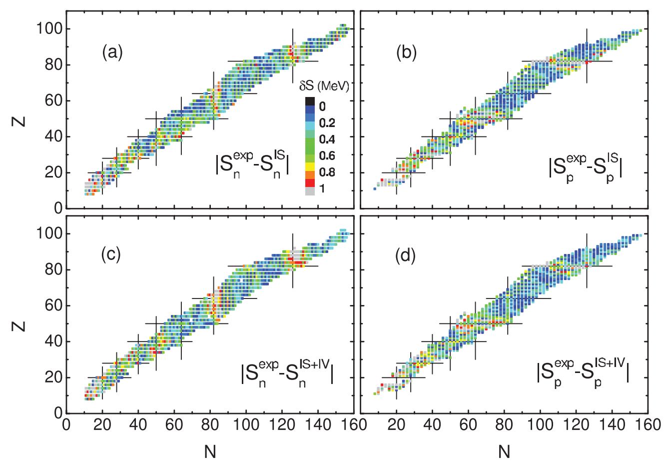

FIG. 3. (Color online) The same as Fig. 2, but for neutron and proton separation energies. See the caption to Fig. 2 and the text for details.

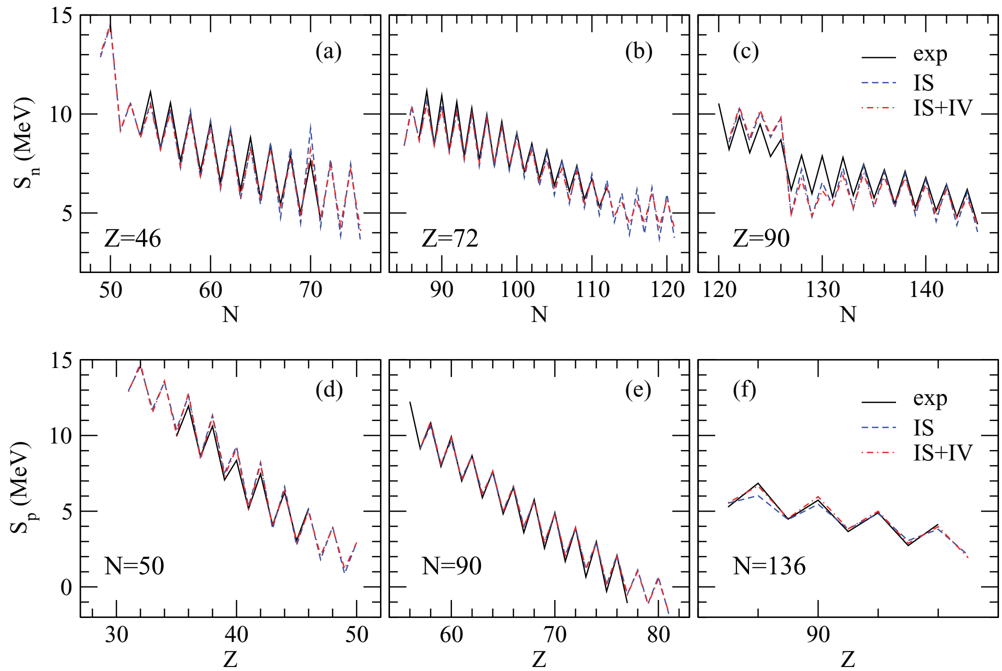

FIG. 4. (Color online) (a)–(c) Neutron separation energies S_n of three isotope chains with $Z = 46$, 72, and 90 calculated by IS and IS + IV interactions in the HF + BCS model (upper panels). (d)–(f) Proton separation energies S_p for $N = 50$, 90, and 136 isotones. Experimental data are taken from Ref. [18]. See text for details.

HF + BCS calculations,

$$\delta E = |E^{\mathrm{exp}} - E^{\mathrm{cal}}|, \tag{7}$$

are shown for both IS and IS + IV pairing interactions in Fig. 2. Figures 2(a) and 2(c) show the values of δE with varying neutron numbers (including both odd and even numbers) for each even Z. Figures 2(b) and 2(d) show the values δE with varying proton numbers (including both odd and even numbers) for each even N.

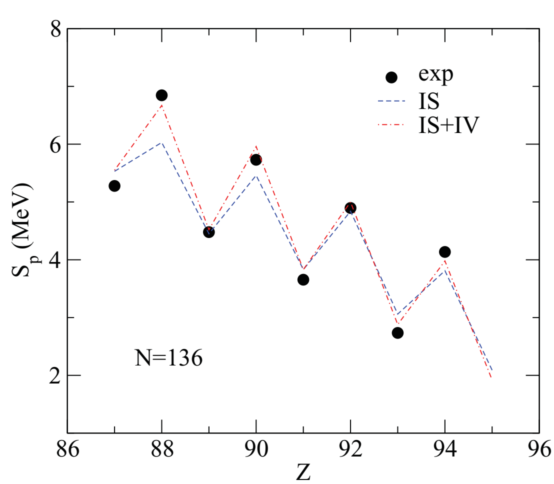

FIG. 5. (Color online) Proton separation energies S_p of $N = 136$ isotones calculated by IS and IS + IV interactions in the HF + BCS model. Experimental data are taken from Ref. [18]. See text for details.

In Fig. 2(b), the binding energy difference between experimental data and calculations with IS pairing is rather large for nuclei along the $Z = 50$ line. This large difference disappears in the case of IS + IV pairing shown in Fig. 2(d). On the other hand, for $N = 82$ nuclei shown in Fig. 2(c), the IS + IV interaction does not work very well compared with the IS interaction shown in Fig. 2(a). As far as the binding energies are concerned, the best results are obtained for $N = 60$–78 and $N = 86$–96 isotones with IS + IV interaction shown in Fig. 2(d).

Separation energy differences between experimental data and HF + BCS calculations for protons and neutrons are

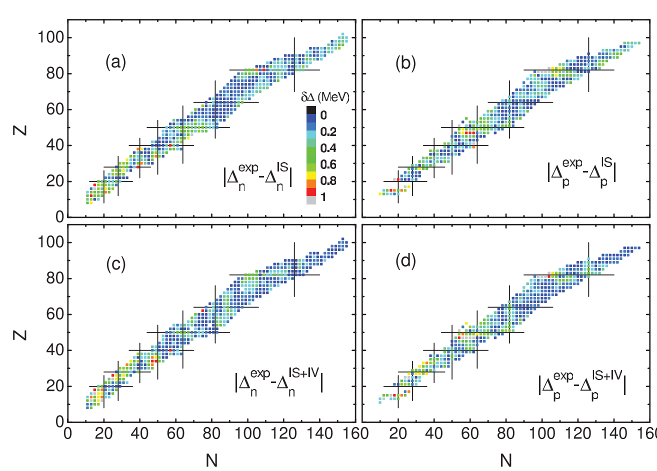

FIG. 6. (Color online) The same as Fig. 2, but for OES for neutrons and protons. See caption to Fig. 2 and text for details.

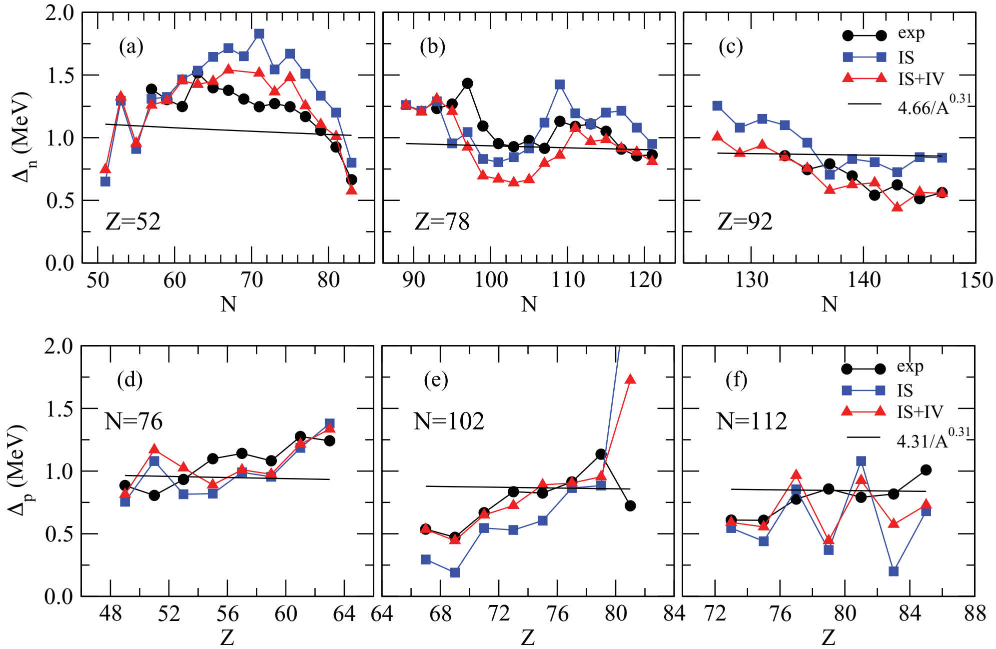

FIG. 7. (Color online) Neutron and proton OES, Δ_n and Δ_p, calculated with the HF + BCS model with IS and IS + IV interactions. Experimental data are taken from Ref. [18]. See text for details.

plotted in Fig. 3. The HF + BCS results for neutron separation energies S_n are reasonable for medium- and heavy-mass nuclei with $N = 60$–120, except near the closed shell $N = 82$. For heavy nuclei with $N = 126$, the calculated results are poorer than in other mass regions. For the proton separation energy S_p, the HF + BCS also gives reasonable results, except in the $Z = 50$ and 82 mass regions.

In order to see the different outcomes between IS and IS + IV pairing interactions, HF + BCS model calculations are shown together with empirical data in Fig. 4. In most cases, the differences between the two pairing interactions are small. However, we can see a clear improvement in the agreement of S_p with empirical data on $N = 136$ isotones with IS + IV pairing in Fig. 5.

The differences in neutron OES Δ_n and proton OES Δ_p between HF + BCS calculations and empirical data are shown in Figs. 6(a) and 6(b) for IS pairing and in Figs. 6(c) and 6(d) for IS + IV pairing. The agreement between HF + BCS calculations and empirical data are good in the overall mass region except for masses with $Z = 50$ and in the small

TABLE II. Average $\Delta^{(3)}$ values for low-isospin and high-isospin nuclei and their difference. See text for details. Exp, experimental data.

	Data set		Low isospin	High isospin	Difference
Neutrons	$Z = 52$	Exp	1.36	1.08	−0.28
		IS	1.52	1.41	−0.11
		IS + IV	1.40	1.19	−0.21
	$Z = 78$	Exp	1.13	0.99	−0.14
		IS	0.96	1.16	0.20
		IS + IV	0.87	0.91	0.04
	$Z = 92$	Exp	0.77	0.56	−0.21
		IS	0.90	0.80	−0.10
		IS + IV	0.70	0.55	−0.15
Protons	$N = 76$	Exp	1.19	0.93	−0.26
		IS	1.13	0.87	−0.26
		IS + IV	1.13	0.98	−0.15
	$N = 102$	Exp	0.96	0.63	−0.33
		IS	0.79	0.39	−0.40
		IS + IV	0.92	0.59	−0.33
	$Z = 112$	Exp	0.87	0.66	−0.21
		IS	0.58	0.61	0.03
		IS + IV	0.67	0.70	0.03

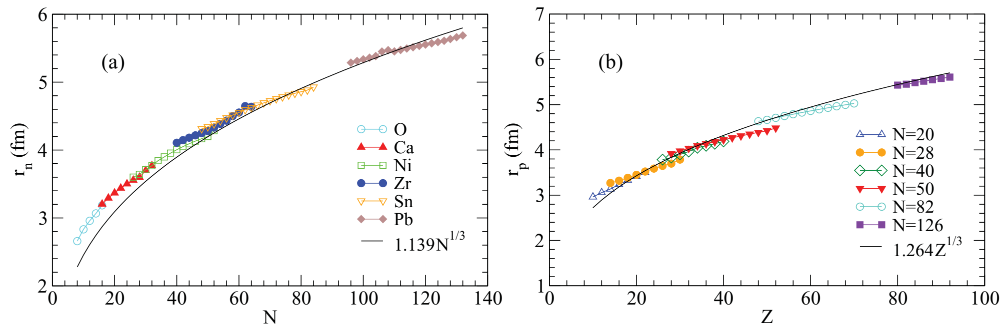

FIG. 8. (Color online) Neutron and proton radii of various isotopes and isotones calculated by means of the HF + BCS model with IS + IV interaction. Solid lines are empirical fits used in Ref. [27]. See text for details.

mass region $A < 60$. To clarify the difference between IS and IS + IV pairing, the OES differences Δ_n are shown in Figs. 7(a)–7(c) for $Z = 52$, 78, and 92 isotopes. The HF + BCS results are compared with the experimental data and also the phenomenological parametrization based on the liquid drop model,

$$\bar{\Delta} = c/A^{\alpha}, \tag{8}$$

with $c = 4.66$ MeV for neutrons and 4.31 MeV for protons and $\alpha = 0.31$, which gives the rms residual of 0.25 MeV [13]. We can clearly see a better agreement of IS + IV results with empirical data for all isotopes. In Figs. 7(d)–7(f), the OES differences Δ_n are shown for $N = 76$, 102, and 112 isotones. The results with IS + IV pairing certainly systematically improve the agreement with empirical data, especially for $N = 102$ isotones. The large increase in the HF + BCS model results at $Z = 81$ is an artifact owing to the shell closure at $Z = 82$. It is interesting to note that the liquid drop formula gives a smooth mass number dependence which reflects well that of very heavy isotones with $N = 112$.

The average gaps $\Delta^{(3)}$ are tabulated for high and low isospins in Table II. Each isotope (isotone) in Fig. 7 is divided into two subsets of almost-equal numbers of nuclei by a cut at some value of $I = (N - Z)/A$. Both the average proton and the average neutron $\Delta^{(3)}$ show smaller values for higher isospins, so that the pairing interaction is weaker for neutron-rich nuclei. The IS + IV interaction reproduces properly the difference in the neutron $\Delta^{(3)}$ between high- and low-isospin nuclei. For proton $\Delta^{(3)}$ also, the IS + IV pairing gives a better account of the isospin effect than the IS pairing.

It was pointed out in Refs. [19] and [20] that the two-body Coulomb interaction reduces the proton gaps by 20%–30%. This Coulomb effect on the pairing gaps is equivalent to about a 10% reduction in the IS-type pairing interaction [21]. On the other hand, for the isospin-dependent pairing case, such as the IS + IV–type one, separate optimization of the proton and neutron pairing interactions will efficiently take into account the reduction in the proton pairing interaction [22].

B. Nuclear radii

Nuclear radii provide basic and important information for various aspects of nuclear structure problems. Proton radii, or, equivalently, charge radii with the correction of finite proton size, can be determined accurately by electron scattering and muon scattering experiments. However, it is difficult to determine the neutron radii of finite nuclei with the same level of accuracy as for the proton radii, although there have been several experimental attempts to determine the difference in the neutron to proton radius [23–25]. It should be noted that the difference in the neutron and proton radii, $\delta r_{np} = r_n - r_p$, is called the neutron skin. It is thought that δr_{np} can provide important constraints on the effective interactions used in nuclear structure study [26].

The neutron and proton radii of various isotopes and isotones are calculated using the HF + BCS model with the two pairing interactions, IS and IS + IV. The results for neutron radii are shown in Fig. 8(a). Because we do not find any appreciable differences between the two pairing interactions in the results, the results of IS + IV interactions are mainly discussed hereafter. The results obtained by the simple empirical formula $r_n = r_0 N^{1/3}$ with $r_0 = 1.139$ fm [27] are also plotted in Fig. 8. In general, the simple formula for r_n agrees well with the HF + BCS results. It is noted that the HF + BCS model gives larger neutron radii for nuclei with $N < 40$ than does the simple formula but smaller radii for nuclei with $N > 120$. The proton radii for $N = 20, 28, 40, 50,$ 82, and 126 isotones are shown as a function of proton number Z in Fig. 8(b). The simple $Z^{1/3}$ dependence is also plotted to follow the formula $r_p = 1.263/Z^{1/3}$. The simple formula in

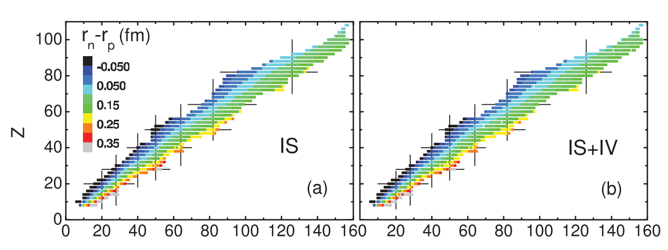

FIG. 9. (Color online) Neutron skin for isotopes and isotones calculated by means of the HF + BCS model with IS and IS + IV interactions. Thin lines indicate closed shells with N (or Z) = 20, 28, 40, 50, 64, 82, and 126. See text for details.

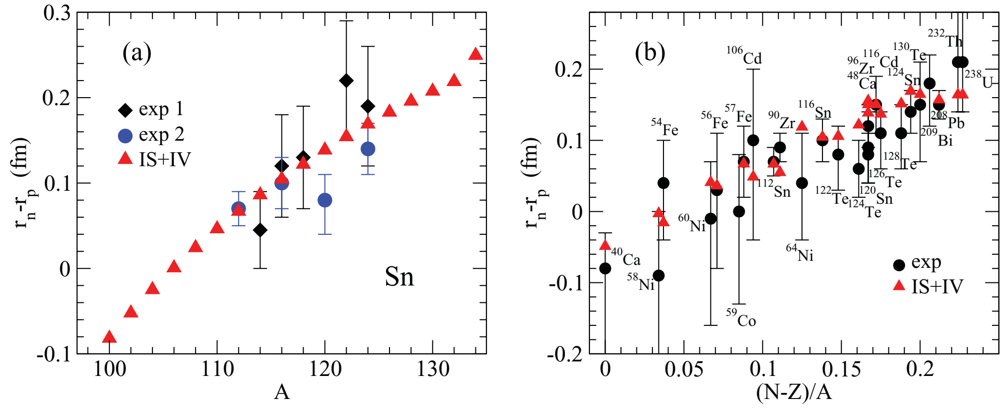

FIG. 10. (Color online) (a) Neutron skin for Sn isotopes obtained with the HF + BCS model with IS + IV interaction. Experimental data are taken from Refs. [23,24]. (b) Neutron skin as a function of isospin parameter $I = (N - Z)/A$ calculated by means of the HF + BCS model with IS + IV interaction. Experimental data are taken from Ref. [25]. See the text for details.

general gives a good account of the HF + BCS data and could be a good starting point for describing the isospin dependence of nuclear charge radii. However, we can see some deviation between the HF + BCS and the simple formula, especially for heavy $N = 50$ and $N = 82$ isotones.

The neutron skin $r_n - r_p$ values calculated by the HF + BCS model with the two pairing interactions are shown in Fig. 9. The neutron skin becomes as large as 0.4 fm near the neutron drip line with $Z < 28$. On the other hand, the neutron skin is at most 0.25 fm in neutron-rich nuclei with $Z > 50$. For proton-rich nuclei, the proton skin becomes 0.1 fm with $Z < 56$ and smaller than 0.05 fm in heavier isotopes, $> Z = 56$. The results of IS and IS + IV pairings are shown in Figs. 9(a) and 9(b), respectively. In general, the two pairing interactions give almost the same results as shown in Fig. 9. However, it is noted that the IS + IV pairing gives somewhat smaller neutron skins than the IS pairing in very neutron-rich nuclei such as ^{136}Sn, ^{150}Ba, and ^{218}Po. The calculated values are compared with empirical data on Sn isotopes obtained from studies of spin-dipole resonances [23] and antiprotonic atoms [24] in Fig. 10(a). The calculated values show reasonable agreement with the empirical data within the experimental error. The isospin dependence of neutron skin is shown in Fig. 10(b) together with empirical values obtained by antiprotonic atom experiments in a wide range of nuclei from ^{40}Ca to ^{238}U. The slope of experimental data as a function of the isospin parameter $I = (N - Z)/A$ is reproduced well by our calculations.

The neutron skin of ^{208}Pb has been discussed intensively in relation to neutron matter properties. Systematic studies of scattering data yield the empirical value $r_n - r_p = 0.17 \pm 0.02$ fm, which is close to another empirical value, $r_n - r_p = 0.15 \pm 0.02$ fm, from a study of antiprotonic-atom systems. A model-independent determination of parity violation experiment at Jefferson Laboratory [26] was proposed and performed recently to obtain the neutron skin of ^{208}Pb. However, the statistics was poor and needs to be improved by accumulation of more data. Our calculated value, $r_n - r_p = 0.157$ fm, is close to the experimental values in the two systematic studies.

IV. SUMMARY AND CONCLUSIONS

In summary, we have studied binding energies, separation energies, and OES using the HF + BCS model with SLy4 interactions together with isospin-dependent pairing (IS + IV pairing) and IS pairing interactions. Calculations have been performed with the EV8odd code for even-even nuclei and also for even-odd nuclei using the filling approximation. For neutron pairing gaps, the IS + IV pairing strength decreases gradually as a function of the asymmetry parameter $[\rho_n(r) - \rho_p(r)]/\rho(r)$. On the other hand, the pairing strength for protons increases for larger values of the asymmetry parameter because of the isospin factor in Eq. (3). The empirical isotope dependence of the neutron OES, $\Delta_n^{(3)}$, is well reproduced by the present calculations with isospin-dependent pairing compared with IS pairing. We also obtain a good agreement between the experimental proton OES and the calculations with isospin-dependent pairing for $N = 50$ and $N = 82$ isotones.

Neutron and proton radii have also been studied using the same HF + BCS model with the two pairing interactions. The two pairing interactions give essentially the same results for the radii except for a few very neutron-rich nuclei. We found systematically large neutron skins in very neutron-rich nuclei, with $|r_n - r_p| \sim 0.4$ fm, while the proton skin is rather small even in nuclei close to the proton drip line because of the Coulomb interaction. The calculated results for the neutron skin show reasonable agreement with the empirical data including the $(N - Z)$ dependence of the data.

We tested the IS + IV pairing for the Skyrme interaction SLy4 and found that the results reproduce the systematic experimental data well. Thus, we confirm a clear manifestation of the isospin dependence of the pairing interaction in the OES in comparison with the experimental data for both protons and neutrons.

ACKNOWLEDGMENTS

This work was partially supported by US DOE Grants No. DE-FG02-08ER41533 and No. DE-FC02-07ER41457 (UNEDF, SciDAC-2), the Research Corporation, JUSTIPEN/DOE Grant No. DEFG02-06ER41407, and the Japanese Ministry of Education, Culture, Sports, Science and Technology by a Grant-in-Aid for Scientific Research under Program No. C(2) 20540277. Computations were carried out on the XT4 Jaguar supercomputer at the Oak Ridge National Laboratory.

[1] A. Bohr, B. R. Mottelson, and D. Pines, Phys. Rev. **110**, 936 (1958).
[2] A. Bohr and B. R. Mottelson, *Nuclear Structure* (Benjamin, New York, 1969), Vol. I.
[3] D. M. Brink and R. Broglia, *Nuclear Superfluidity, Pairing in Finite Systems, Cambridge Monographs on Particle Physics, Nuclear Physics and Cosmology,* Vol 24 (Cambridge University Press, Cambridge, 2005).
[4] M. Bender, P.-H. Heenen, and P.-G. Reinhard, Rev. Mod. Phys. **75**, 121 (2003).
[5] M. V. Stoitsov, J. Dobaczewski, W. Nazarewicz, and P. Borycki, Int. J. Mass Spectrom. **251**, 243 (2006).
[6] S. Hilaire, J.-F. Berger, M. Girod, W. Satula, and P. Schuck, Phys. Lett. B **531**, 61 (2002).
[7] W. Satula, J. Dobaczewski, and W. Nazarewicz, Phys. Rev. Lett. **81**, 3599 (1998).
[8] T. Duguet, P. Bonche, P.-H. Heenen, and J. Meyer, Phys. Rev. C **65**, 014311 (2001).
[9] J. Margueron, H. Sagawa, and K. Hagino, Phys. Rev. C **76**, 064316 (2007).
[10] M. Yamagami and Y. R. Shimizu, Phys. Rev. C **77**, 064319 (2008).
[11] P. Bonche, H. Flocard, and P. H. Heenen, Comput. Phys. Commun. **171**, 49 (2005).
[12] G. Bertsch and C. A. Bertulani, unpublished. EV8odd code available upon request.
[13] G. F. Bertsch, C. A. Bertulani, W. Nazarewicz, N. Schunck, and M. V. Stoitsov, Phys. Rev. C **79**, 034306 (2009).
[14] C. A. Bertulani, H. F. Lu, and H. Sagawa, Phys. Rev. C **80**, 027303 (2009).
[15] The Universal Nuclear Energy Density Functional, a SciDAC project. Available at: [http://unedf.org].
[16] T. Duguet, P. Bonche, P. H. Heenen, and J. Meyer, Phys. Rev. C **65**, 014310 (2001).
[17] J. Margueron, M. Grasso, G. Colò, S. Goriely, and H. Sagawa, J. Phys. G **36**, 125103 (2009).
[18] G. Audi, A. H. Wapstra, and C. Thibault, Nucl. Phys. A **729**, 337 (2003).
[19] M. Anguiano, J. L. Egido, and L. M. Robledo, Nucl. Phys. A **683**, 227 (2001).
[20] T. Lesinski, T. Duguet, K. Bennaceur, and J. Meyer, Eur. Phys. J. A **40**, 121 (2009).
[21] H. Nakada and M. Yamagami, Phys. Rev. C **83**, 031302(R) (2011).
[22] M. Yamagami, forthcoming.
[23] A. Krasznahorkay *et al.*, Phys. Rev. Lett. **82**, 3216 (1999).
[24] A. Trzcinska, J. Jastrzebski, P. Lubinski, F. J. Hartmann, R. Schmidt, T. von Egidy, and B. Klos, Phys. Rev. Lett. **87**, 082501 (2001).
[25] J. Jastrzebski *et al.*, Int. J. Mod. Phys. E **13**, 34 (2004).
[26] C. J. Horowitz and J. Piekarewicz, Phys. Rev. C **64**, 062802 (2001).
[27] Jie Meng *et al.*, Prog. Part. Nucl. Phys. **57**, 470 (2006).